A circular switched parasitic array with directors for LoRa applications at 868 MHz

Lukas Reinhold,✉ Casper Wasle, and Alexander Kölpin
Institute of High-Frequency Technology, TUHH, Hamburg, Germany
✉ E-mail: lukas.reinhold@tuhh.de

The integration of directive elements into a circular switched parasitic array at 868 MHz is presented. The typical usage of reflective parasitic monopoles is supplemented with additional, shorter monopole elements which are positioned closer to the central active monopole to induce directive behaviour. This allows for more degrees of freedom with the steering of the antennas beam and to increase the gain of the antenna. This leads to a greater flexibility of the system and enables power reduction of the amplifiers for enhanced battery life time. The design and configuration of a circular switched parasitic array with directive elements is shown and a prototype is built for validation.

Introduction: Circular switched parasitic arrays (CSPA) are an approach for a steerable antenna with no moving parts. An arrangement of passive elements around a single active element forms the beam of the overall structure by placing specific impedances at the passive elements ports [1]. A circular arrangement allows for steerability in one plane, if the loads at the ports are switchable or tunable. As only one antenna element needs to be actively fed, the feed structure requires only one feed path with active radio frequency components. The directivity of the antenna can be further increased by placing monopole elements on a ground plane and extending this surface downwards with a skirt [2] (see Figure 1). A secondary circular metal structure can be placed above the elements to limit upwards radiation and increase vertical beamforming [3].

In this letter the integration of directive elements into a CSPA for LoRa applications at 868 MHz is presented. Combined with the conventional reflective elements of a CSPA, the functionality of a Yagi–Uda antenna can be replicated in several orientations. The additional directive elements allow for increased antenna gain and a finer steerability of the antennas main beam. The presented antenna is designed to minimize the power consumption of the whole communication system by lowering the amplification and its power requirements while compensating this by a higher, steerable antenna gain. The antenna is optimized to switch between several efficient directive links. This is especially valuable for sensor network gateways which have end nodes arbitrarily distributed over a large area and put a focus on power efficiency.

Integration of directors into the CSPA-layout: A Yagi–Uda antenna places directive and reflective elements in a line with a single active element to generate a directed radiation pattern [4]. The reflective elements are placed along the opposite direction of radiation, are usually longer than the active element and often have a distance of below $\lambda/2$ to the active element. Directive elements are placed along the desired radiation direction. Usually multiple directive elements are used with periodic spacing in between them but there is a diminishing gain for a large quantity of elements. The distances are chosen so, that the parasitic, re-radiated fields of the directive elements constructively interfere in the desired direction of radiation. In contrast a CSPA conventionally consists of a single active element in its center and a circle of several parasitic elements placed in a circle, often with a radius of about $\lambda/4$ around it. More elements in the circle allow for a finer control of the direction of the formed beam but also increase the complexity of the system. If the spaces between the elements are set too small, undesired coupling effects between them may be introduced.

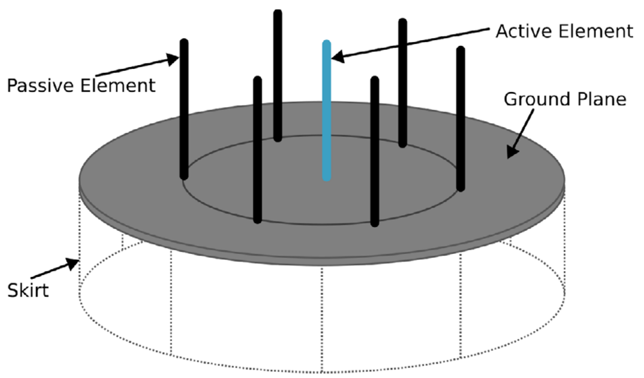

Fig. 1 *Shown is the basic structure of a CSPA antenna. Below it a solid metal skirt for improved beamforming is sketched*

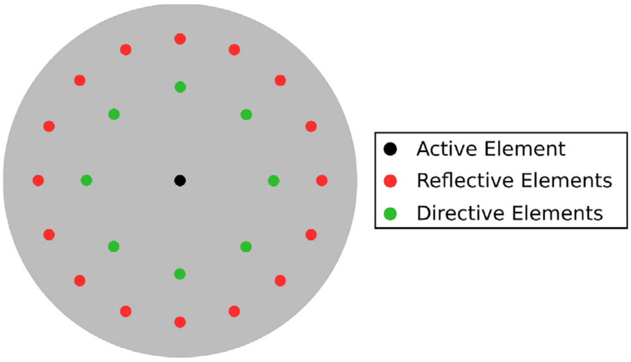

Fig. 2 *The schematic layout of the monopole elements of the CSPA on a circular metal plate is shown as a top down view. The layout encompasses 1 active element, 8 directive elements in an inner ring and 16 reflective elements in an outer ring*

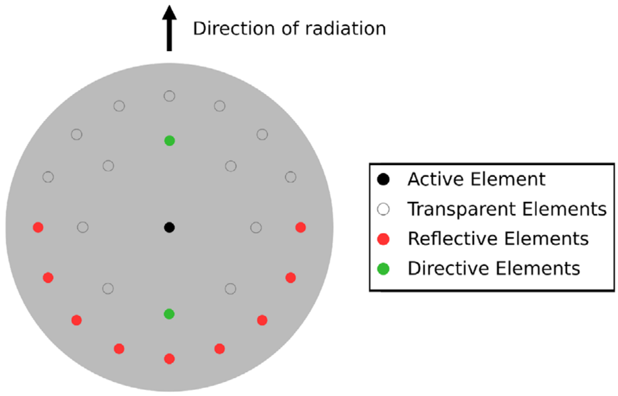

Fig. 3 *Shown is the main configuration of the designed CSPA for maximum gain with 2 directive elements and 9 reflective elements turned on*

For the CSPA presented in this letter, an iterative approach for the integration of directors in the antenna is chosen. Initially, the design of a Yagi–Uda antenna is replicated with one reflector, one director and the active element between the parallel plates of the antenna. The lengths and spacings of the director, reflector, and active element where based off typical values for a Yagi–Uda antenna [4]. Combinations of multiple numbers of reflectors and directors in different arrangements were simulated, and each iteration was optimized with regard to maximum realized gain in the simulation software. Each combination is constrained to have a circular symmetry to ensure the antenna can switch the same pattern in multiple directions. The best combination of elements obtained by this process with regard to realized gain is shown in Figure 2. In a CSPA, each reflector and director element can either be in a transparent or off state or in an interactive or on state. This allows the depicted pattern to be switched into eight different directions.

The best found configuration in terms of realized gain is shown in Figure 3 with 2 directive elements on, one in front of and one behind the active element along the desired direction of radiation. Reflective elements are turned on in a semicircle behind the active element. Simulations show a maximum realized gain of 9.7 dBi and a half power beam

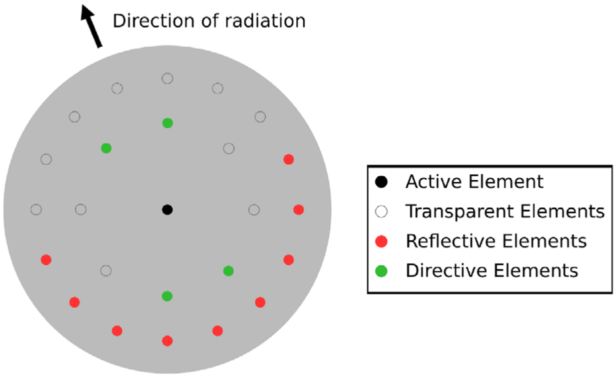

Fig. 4 *Shown is the microstep configuration of the designed CSPA for steering the main lobe of the antenna in the 8 direction least covered by the main configurations. Four directive elements and 9 reflective elements are turned on*

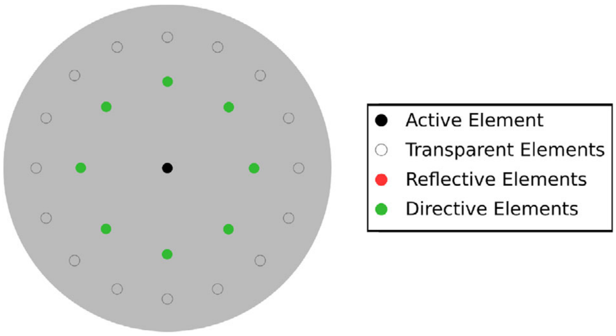

Fig. 5 *Shown is the quasi-omnidirectional configuration designed to radiate power as evenly as possible along the horizontal plane of the antenna. All 8 directive elements and no reflective elements are turned on*

width of about 70° in the horizontal plane. This presents approximately a 2 dB gain increase above previous simulations without directive elements. The state of the directors and reflectors can be changed by switching between an open circuit condition at the parasitic elements port for the off state and a short circuit condition for the on state. Semiconductor switches for the appropriate frequency range are used for this function [5].

This optimal configuration can be rotated around the active element in 8 steps of 45° each, limited by the number of directive elements. This leaves 8 dips in between these main directions where either adjacent beam-configuration only realizes a gain of about 7 dBi. Additional configurations were found, which form signal beams in between the main steps. 4 directive elements can be turned on, 2 in front of and 2 behind the active element. The configuration is shown in Figure 4. The directing effects of the 2 elements adjacent to each other overlap and the direction of the resulting lobe is in between them. The antenna gain in this microstep configuration is about 1 dB lower than the maximum gain in the main configuration but still about 2 dB higher than any main configuration can cover in these directions. Combining both configurations the main beam of the antenna can be moved into 1 of 16 horizontal directions in 22.5° steps and cover any direction with a gain variation of about 1 dB. A $\lambda/4$-monopole antenna radiates fields with a linear polarization. As all conductive components of the CSPA are either parallel or orthogonal to the active element, the same polarization characteristics are expected by the CSPA. Simulations of the designed antenna corroborate this.

In theory, all elements can be turned off to turn the CSPA into a omnidirectional antenna in the horizontal plane. This however leads to a strong mismatch between the active element and the space between the metal plates, as the CSPA is optimized and matched for operation with two directive elements turned on. Instead, all directive elements can be turned on and all reflective elements can be turned off. This configuration is shown in Figure 5. The fields of the active element couple into the directive elements which improves matching but the directing effects of the inner elements roughly cancel each

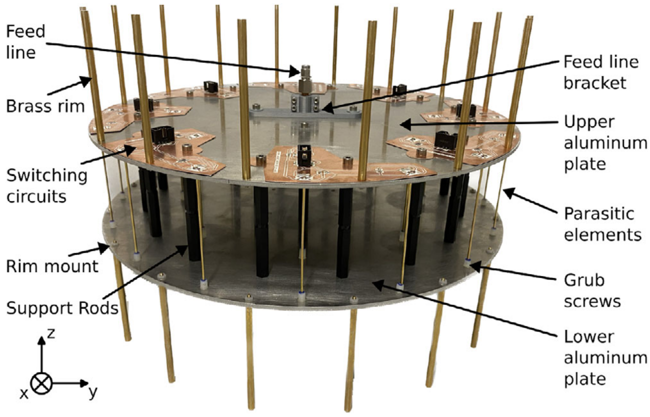

Fig. 6 *Shown is the prototype of the CSPA with the major components marked*

other out. The result is a quasi-omnidirectional radiation characteristic with some slight variations in the realized gain between 2.5 and 2.2 dBi correlating to the positions of the support structure of the antenna.

The antenna design: The presented CSPA was simulated and optimized in CST Microwave Studio and a prototype was manufactured. The build prototype is shown in Figure 6. The antenna is build in-between two circular aluminium plates. The upper plate forms the ground plane for all monopole elements. Printed circuit boards with the switching circuits are mounted on its outer surface and the feed line to the active element is at its center. The lower plate has no conductive connection to the upper plate. It shapes the radiation pattern to minimize radiation towards the bottom of the antenna in negative z-direction. This approach for two parallel metal plates to form a beamforming structure is shown in Ref. [3].

Additional brass rods with a length of $\lambda/4$ are added along the border of both plates pointing outwards. The aperture of the antenna is thereby increased along the height of the CSPA without increasing the wind load or the weight of the antenna notably. This increase the CSPAs directivity in the vertical plane as shown in Ref. [2]. The length of the rods can be increased by a multiple of $\lambda/2$ to slim the radiated beams vertically. This however further increases the space required to mount the antenna and the longer rods are harder to affix to the CSPA in a stable manner.

20 support rods made from polyamide keep an even distance of 80 mm between the two aluminium plates. They are placed in spaces as far away from the monopole elements as possible to minimize dielectric detuning of the elements and to not interfere with the switching circuits on the circuit boards.

The active element is made from a semi-rigid coaxial cable. The outer shielding and the dielectric are stripped from its tip to expose the inner conductor for a length a little smaller than $\lambda/4$ as the active monopole antenna in the center. The remaining dielectric and shielding are used to isolate the inner conductor against the aluminium plate and to attach a SMA connector for the feed line.

The 24 parasitic elements are slim brass rods with a diameter of 1.5 mm. Segments of the semi-rigid cable dielectric and shielding are used to press fit the rods into the upper aluminium plate as depicted in Figure 7. Two parallel radio-frequency switches are used per parasitic element to reduce the current per switch and introduce redundancy. The open load is realized as an open stub line and the shorted load as a via connecting the upper copper layer of the printed circuit board to the aluminium plates, which is the ground plane to the monopole elements. The semiconductor single-pole, double-throw switches connect the feed point to either the short or the open load.

Grub screws made from polyamide are threaded through the lower plate to stabilize the lower end of the monopole elements. The proximity of the lower metal plate to the monopole elements introduces capacitive coupling which detunes the elements. The brass rods were shortened appropriately. The active element is about 73 mm long, the directive

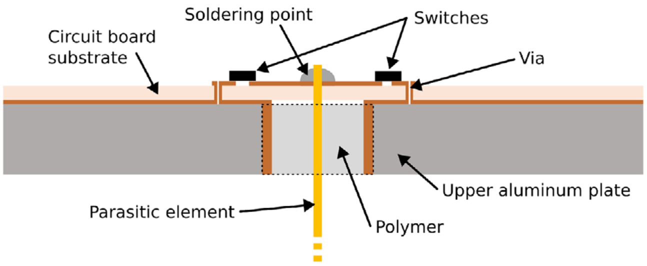

Fig. 7 *The transition of a parasitic element through the upper aluminium plate to the switching circuit is shown. Copper is drawn in dark brown. The inserted mantle and dielectric of the semi rigid cable is marked with a dashed rectangle*

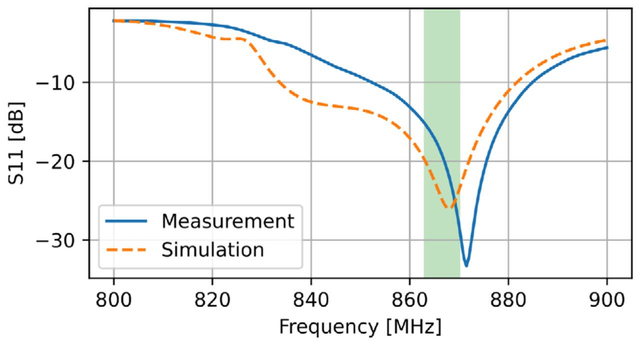

Fig. 8 *The measured input reflection S11 is shown and compared to the simulation results. The desired frequency band between 863 and 870 MHz is marked with a green rectangle*

elements in the inner ring are 72 mm long and the reflective elements of the outer ring are about 75 mm long.

Measurements: The input reflection of the CSPA prototype was measured in an anechoic chamber with a network analyser calibrated to the connector plane. The results are shown in Figure 8. Compared to the simulation results the measured resonance frequency is about 3 MHz higher. The measurements show a good match at the desired frequency band from 863 to 870 MHz with a input reflection of −15 dB or less. The shift of the resonant frequency is probably introduced by slight inaccuracies in the monopole elements lengths due to manufacturing tolerances.

The radiation pattern of the CSPA was validated in an anechoic chamber. A network analyser was calibrated using the three antenna method with commercially available mobile-network antennas as reference antennas. For the measurement, the CSPA was mounted on a rotatable tower to align the CSPA along the configurable directions of radiation. The antenna could also be rotated around its direction of radiation to validate the polarization characteristics.

The Figures 9 and 10 show the measured radiation characteristic of the designed CSPA in its main configuration with two directors on (compare Figure 3). The simulated values are represented by a dashed line for comparison. A horizontal cut through the far-field radiation pattern is shown in Figure 9. The depicted measurement run was done with a sideways mounted antenna with the tower located at −90° to include all side-lobes. The right half of the graph is a mirror image of the left, added for clarity. The maximum measured realized antenna gain is about 8.0 dBi which is 1.7 dB below the simulated value. The half power beam width is 70° in the horizontal plane.

Figure 10 shows the vertical cut through the far-field of the main beam of the antenna. The half power beam width is about 68° in this plane. Both far field cuts show a minor reduction in realized gain compared to the simulation while the shape of the main beam matches well. The change in gain is most likely due to additional losses introduced by manufacturing imprecision resulting in a slight detuning of the monopole elements resonances. Additional material losses, especially in the printed circuit board, which were not accounted for in the simulation model may also influence the results.

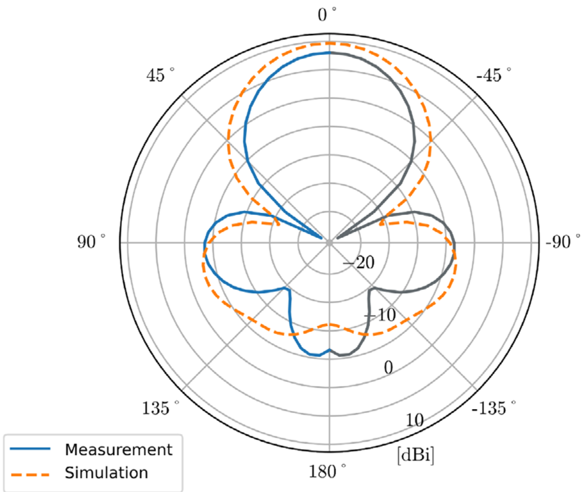

Fig. 9 *The measured and simulated far-field characteristics of the designed CSPA in the horizontal plane*

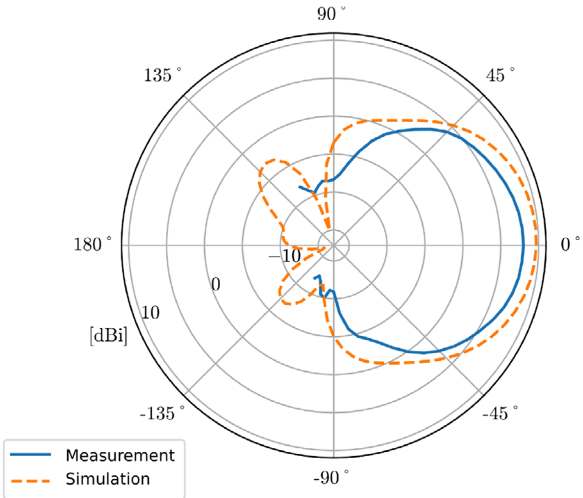

Fig. 10 *The measured and simulated far-field characteristics of the designed CSPA in the vertical plane*

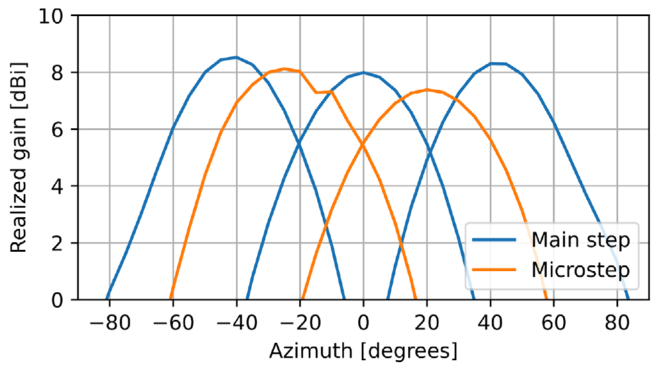

Fig. 11 *Five mainlobes in the horizontal plane are shown for adjacent antenna configurations to compare microstep and main step configurations*

The CSPA was also rotated to measure the far-field characteristics of the different configurations. This was done to evaluate the symmetry of the manufactured antenna and to verify the benefits of the microstep configurations. The main lobes of five adjacent configurations are shown in Figure 11. It can be seen, that the lobes with microstep configurations fill in gaps which are not covered by the main lobes as well and smooth out the antennas gain over the covered angles. Instead of a variation in gain over the angles of about 2.5 dB the variation can be reduced to about 1 dB using the microstep configurations.

Conclusion: It was shown that directive elements can be introduced into a circular switched parasitic array to improve its radiation characteristics. A ring of directive elements was introduced in addition to the typical ring of reflective elements. A realized gain of 9.7 dBi was shown to be possible in simulations and a gain of 8.0 dBi was measured on the manufactured prototype. Selectively turning the parasitic elements on, steers the main beam of the antenna in 16 evenly spaced steps along the horizontal plane. This was achieved by a Yagi–Uda inspired main configuration of directive and reflective elements and a microstep layout with two adjacent directive elements turned on.

Author contributions: **Lukas Reinhold**: Conceptualization; investigation; validation; writing—review and editing. **Caspar Wasle**: Conceptualization; data curation; formal analysis; investigation; software; validation; writing—review and editing. **Alexander Koelpin**: Funding acquisition; supervision; writing—review and editing.

Acknowledgement: Funded by the German Federal Ministry of Education and Research under grant 01LC1903L.

Conflict of interest statement: The authors declare no conflicts of interest.

Data availability statement: The data that support the findings of this study are available from the corresponding author upon reasonable request.

Received: *25 April 2024* Accepted: *24 May 2024*
doi: 10.1049/ell2.13247

References

1 Harrington, R.: Reactively controlled directive arrays. *IEEE Trans. Antennas Propag.* **26**(3), 390–395 (1978)
2 Panagiotou, S.C., Dimousios, T.D., Capsalis, C.N.: Analysis and design of a broadband circular switched parasitic array above finite plate and finite plate with skirt. In: International Conference on Electromagnetics in Advanced Applications, pp. 727–730. IEEE, Piscataway, NJ (2007)
3 Bertuch, T.: A circular switched parasitic array antenna for high power data link applications. In: 3rd European Conference on Antennas and Propagation, pp. 2483–2487. IEEE, Piscataway, NJ (2009)
4 Viezbicke, P.P.: Yagi Antenna Design. National Institute of Standards and Technology, Gaithersburg, MD (1976)
5 Locker, C., Landsberg, A., Bertuch, T.: Solid sate vs. micro relay-switches employed in a circular switched parasitic array antenna. In: 9th European Conference on Antennas and Propagation (EuCAP), pp. 1–5. IEEE, Piscataway, NJ (2015)